JOURNAL OF CATALYSIS **138**, 562–569 (1992)

Oxidation of Carbon Monoxide over Cobalt and Aluminium Substituted Y–Ba–Cu–O Perovskites

J. C. OTAMIRI,* J. E. CROW,† AND S. L. T. ANDERSSON*

**Department of Chemical Technology, Chemical Center, University of Lund, P.O. Box 124, S-221 00 Lund, Sweden, and †Center for Materials Research and Technology, The Florida State University, Tallahassee, Florida 32306-3016*

Received May 17, 1991; revised June 15, 1992

CO oxidation over $YBa_2Cu_{3-\delta}Me_\delta O_{6+x}$, where Me is Co or Al, has been studied. The activity for CO oxidation decreases with increasing degree of substitution in the B site, in the case of substitution both with a more active element (Co) and with an inactive element (Al). The active site is believed to consist of –Cu–( )–Cu–, where ( ) can be an oxygen species O or an oxygen vacancy [ ]. Dilution of this site with less active –Cu–( )–Me– results in a lower activity. Nitrogen-annealed samples show a considerably higher activity than oxygen-annealed samples. Oxidation–reduction experiments suggest that bulk influences such as oxygen diffusion and filling of vacancies also affect activity.

INTRODUCTION

The $YBa_2Cu_3O_{6+x}$ cuprate perovskite system (YBCO) is investigated concerning its physical and electronic properties (*1–3*). Comparatively little attention is focussed on its catalytic properties, although it shows activity for a variety of reactions (*4–16*). Further catalytic investigations involving the YBCO system are important considering the following facts. The surface is known to react with atmospheric water and CO_2, forming surface degradation products (*17, 18*). It was recently suggested that the degraded thin surface acts as a supported active phase, while the intact bulk YBCO acts as the support (*11*). The reactivity is then influenced by changes both in the bulk and at the surface. Furthermore, the formal charge on Cu based on the stoichiometric composition and oxygen content should vary between 1+ and 3+. It is, however, believed that the excess charge is located on the oxygens in the form of positive holes and not as formal Cu^{3+} species (*19–22*). Consequently, reactive oxygen species may be present in these materials and the variable valence state of Cu can induce different types of reactions depending on the conditions. Indeed, this behavior is believed to be responsible for the total combustion of toluene at high pressures of O_2, and selective (amm)oxidation at low pressures (*5, 6, 12*). Substitution of Cu by other transition metals influences the physical and catalytic properties and we found a decreased ammoxidation activity with the addition of Zn (*11*). This may be expected, considering that a rather inactive component is added. In this work we therefore compare the effects of substitution with an active component, Co, and an inactive component, Al. Both are believed to enter the lattice with 3+ valence and to substitute for the Cu-chain sites (*23, 24*). Beyond $\delta = 0.09$–0.15 in $YBa_2Cu_{3-\delta}Me_\delta O_{6+x}$, the structure switches from orthorhombic to tetragonal and there is an enhanced oxygen occupancy in the vicinity of the chains (*23, 24*). Oxygen vacancies are affected by these replacements, and their role may be important. In a previous investigation the activity for CO oxidation could be correlated to the *x*-value (*16*), which would be interesting to correlate also in this

0021-9517/92 $5.00

study where the x-value is influenced by the varied substitutions.

EXPERIMENTAL

Preparation and Characterization of Samples

Samples were prepared by heating stoichiometric mixtures of pure and well ground CuO, Y_2O_3, $BaCO_3$, Co_3O_4, and Al_2O_3 at 920°C for 24 h. The resulting mixtures were several times reground, pelletized, and fired again at 920°C. The samples denoted as $YBa_2Cu_{3-\delta}Me_\delta^{ox}O_{6+x}$ (in short $YBCMe_\delta^{ox}$) were then finally annealed in O_2 at 500°C for several hours, while the samples denoted $YBa_2Cu_{3-\delta}Me_\delta^{red}O_{6+x}$ (in short $YBCMe_\delta^{red}$) were annealed in nitrogen at similar conditions. Me stands for either Co or Al. The x-values for fresh and used catalysts were determined by iodometric titrations as described elsewhere (*13, 16*). The specific surface areas for the perovskite samples were between 0.4 and 0.5 m^2/g, for CuO 3.6 m^2/g, and for Co_3O_4 1.7 m^2/g. XRD analysis was performed on a Philips X-ray powder diffractometer equipped with a diffracted beam monochromator using Cu$K\alpha$ radiation from a 4-kW X-ray generator (PW1730) operated at 40 kV and 20 mA. XPS studies were carried out on a Kratos XSAM800 instrument by procedures described earlier (*6, 18*). Sensitivity factors used were Cu $2p_{3/2} = 2.65$, Co $3p = 0.32$, and Al $2s = 0.21$.

Catalytic Activity Measurements

The activity measurements were carried out in a conventional microflow reactor which was operated at atmospheric pressure. In each experiment, the catalyst bed was loaded with about 0.7 g of catalyst mixed with 2 g of inert quartz. $YBCMe_\delta^{ox}$ was pretreated in the reactor by heating in O_2 at 400°C for about 1 h, followed by cooling to 200°C and catalytic measurements between 200 and 300°C. $YBCMe_\delta^{red}$ was pretreated by heating in N_2 at 400°C for about 1 h and then cooled to 160°C, followed by catalytic measurements between 160 and 250°C. The *in situ* annealing is considered to be a continuation of the last step in the sample preparation. The total gas flow rate was 24 liter/h. Over $YBCMe_\delta^{ox}$ samples, the partial pressures of CO and O_2 were kept constant at 4 and 166 Torr, respectively, but for $YBCMe_\delta^{red}$ they were maintained at 4 and 16 Torr, respectively. At the end of these treatments, samples were cooled and transferred for XPS the same day and also for chemical analysis. CO and CO_2 formed during reaction were analysed with an on-line gas chromatograph.

RESULTS

Oxygen Stoichiometry and Structural Composition

X-ray diffraction (XRD) measurements show that the Co-substituted samples are pure single phase samples, both before and after use in the catalytic oxidation of CO. The Al-substituted samples are less pure, with the main impurity Y_2BaCuO_5 in concentrations of a few percent. The fresh, oxygen-annealed samples $YBCMe^{ox}$ are orthorhombic, but after use shifts in peak heights indicate formation of the tetragonal phase. Both fresh and used nitrogen-annealed samples, $YBCMe^{red}$, are of the tetragonal phase. Similar observations are made by the oxygen titration results, see Table 1. The fresh, oxygen-annealed samples, $YBCMe^{ox}$, have x-values from 0.61 to 0.85, while the fresh, nitrogen-annealed samples $YBCMe^{red}$ have x-values from 0.48 to 0.60. All used samples have lower x-values than before use and range from 0.37 to 0.67.

Surface analysis by X-ray photoelectron spectroscopy (XPS) showed quantitative variations mainly in Cu, Co, and Al, as presented in Table 1 as the δ-value. For Co-substituted samples these are in reasonable agreement with the nominal values, whereas for Al-substituted samples large deviations occur. Thus for $Al_{0.24}$ the largest δ-value by XPS is obtained. The nitrogen-annealed $YBCCo^{red}$ samples were also analyzed after use in oxidation of CO. The main effect observed was a varied valence state of copper, with predominance of Cu(II) and increasing content of Cu(I) with decreasing oxygen pressures, which was followed by the Cu $2p_{3/2}$ satellite to the main line intensity ratio (*18*). Thus, after use of $YBCCo_{0.12}^{red}$ at p_{O_2} = 4–8 Torr this ratio was 0.33, indicating about 50% Cu(II). Corresponding data were as follows: For $YBCCo_{0.24}^{red}$ p_{O_2} = 8 Torr, 0.41 and 60% Cu(II); for $YBCCo_{0.36}^{red}$ p_{O_2} = 16 Torr, 0.46 and 70% Cu(II); and for $YBCCo_{0.48}^{red}$ p_{O_2} = 166 Torr, 0.55 and 85% Cu(II). The Co $2p$ core lines could not be observed due to overlap with the Ba $3d$ core lines. Therefore, the much weaker Co $3p$ line was used for quantification purposes. Due to its broad and weak structure, precise measurement of its binding energy was not successful, and hence we could not determine the valence state of Co. The Ba $3d$ and O $1s$ core lines gave binding energies in agreement with earlier results showing the presence of a degraded surface layer over the YBCO samples (*17*, *18*).

Catalytic Activity

The conversion of CO as a function of temperature over the Co-substituted catalysts is shown in Fig. 1. Similar results for the aluminium-substituted catalysts are shown in Fig. 2. A common pattern observed for all the substituted materials is that the activity over $YBCMe_{\delta}^{red}$ is much higher than that over $YBCMe_{\delta}^{ox}$ and similar conversions are obtained at considerably lower temperatures. It is also evident that conversion is higher over Al-substituted than over Co-substituted samples. Concerning activity of the pure components, measurements showed that it was too low over Al_2O_3 to measure, while it was considerably higher over Co_3O_4 than over CuO. Thus, to achieve an activity of 15 μmol · m^{-2} · min^{-1} a temperature of 140°C was required for CuO, whereas it was 120°C for Co_3O_4 at 166 torr O_2 and 4 torr CO in both cases. The main impurity in the Al-substituted samples, Y_2BaCuO_5, requires about 400°C to achieve the same activity at these conditions. In the concentrations detected by XRD, a few per cent, its influence on the various samples should result in a negligibly reduced activity. The apparent activation energies calculated from activities measured below 20% conversion are 16–17 kcal/mole for YBC Co^{ox}, 9–10 kcal/mole for $YBCCo^{red}$. The order is reversed for Al-substituted samples with 10–11 kcal/mole for $YBCAl^{ox}$ and 21–24 kcal/mole for $YBCAl^{red}$. On the whole, the apparent activation energy is rather constant at a varied degree of substitution.

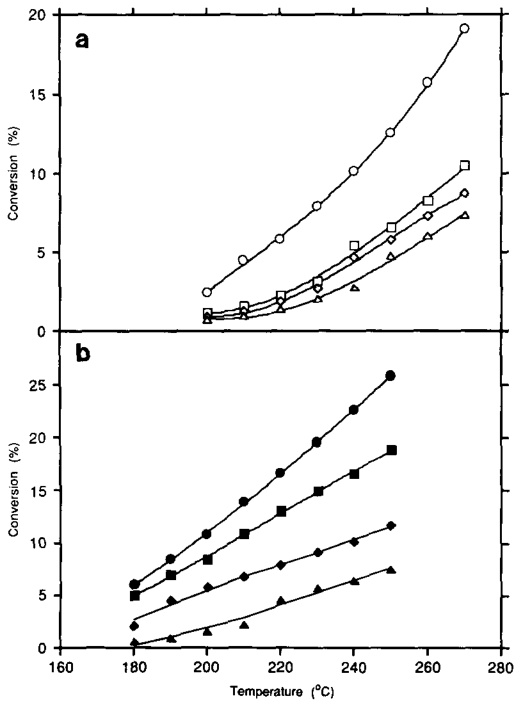

FIG. 1. Conversion of carbon monoxide over cobalt-substituted YBCO perovskites as a function of temperature. (a) $YBa_2Cu_{3-\delta}Co_{\delta}^{ox}O_{6+x}$: (o) $\delta = 0.12$; (□) $\delta = 0.24$; (◇) $\delta = 0.36$; (△) $\delta = 0.48$ (p_{CO} = 4 Torr, p_{O_2} = 166 Torr). (b) $YBa_2Cu_{3-\delta}Co_{\delta}^{red}O_{6+x}$: (●) $\delta = 0.12$; (■) $\delta = 0.24$; (◆) $\delta = 0.36$; (▲) $\delta = 0.48$ (p_{CO} = 4 Torr, p_{O_2} = 16 Torr).

The influence of the degree of substitution on the reaction rates is shown in Table 1. The rates are from different temperatures for oxygen- and nitrogen-annealed samples. Cobalt samples show a decrease in activity with an increase in nominal cobalt content.

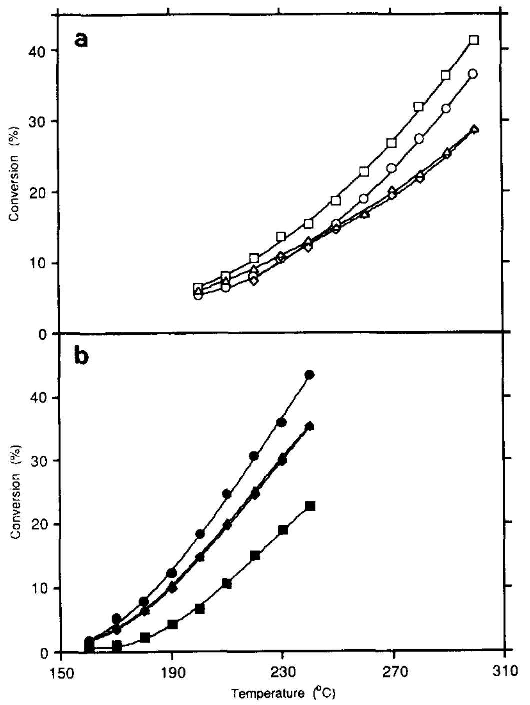

FIG. 2. Conversion of carbon monoxide over aluminium-substituted YBCO perovskites as a function of temperature. (a) $YBa_2Cu_{3-\delta}Al_\delta^{ox}O_{6+x}$: (○) $\delta = 0.12$; (□) $\delta = 0.24$; (◇) $\delta = 0.36$; (△) $\delta = 0.48$ ($p_{CO} = 4$ Torr, $p_{O_2} = 166$ Torr). (b) $YBa_2Cu_{3-\delta}Al_\delta^{red}O_{6+x}$: (●) $\delta = 0.12$; (■) $\delta = 0.24$; (◆) $\delta = 0.36$; (▲) $\delta = 0.48$ ($p_{CO} = 4$, Torr, $p_{O_2} = 16$ Torr).

Except for the different behavior of both $YBCAl_{0.24}$ samples, the effect of Al substitution is similar, although less pronounced.

Figure 3 shows the response of time on stream in conversion of CO to step changes in the O_2 pressure for some reduced and oxidized samples. The conversion over $YBCCo^{ox}$ samples (pretreated in oxygen) passed through an optimum with time on stream during CO oxidation at 0 Torr oxygen. After 85 min the oxygen pressure was increased to 166 Torr, resulting initially in a doubled CO conversion, which gradually decreased with increasing time on stream. The conversion over $YBCCo^{red}$ samples (pretreated in nitrogen) showed a low conversion, decreasing with time, at the initial measurement at an oxygen pressure of 166 Torr. The step decrease in oxygen pressure to 8 Torr after 85 min. time on stream resulted in a slowly increasing conversion, which after 2 h is about 4–5 times higher than initially. Thereafter, the conversion decreases with time.

DISCUSSION

The surface of the YBCO system is believed to differ from the bulk due to reaction with atmospheric water and CO_2 (*17, 18*). Thus, it might be rightly argued that the catalysis over this sytem should be interpreted strictly in terms of the surface structures and the properties associated with them. What seems to be interesting here is that, following several systematic studies (*4–6, 11, 16*), we have observed that changes in the bulk structure of the YBCO system affects oxidation catalysis strongly. In order to be able to understand the underlying mechanisms involved in these oxidation processes, it will be worth while to consider the relationship between the oxygen stoichiometry, oxygen vacancy ordering, crystal structure, and surface properties.

Crystal and Structural Composition

The crystal structures of the YBCO compounds can be considered to be made

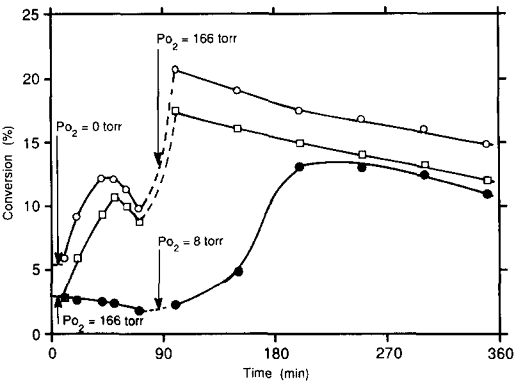

FIG. 3. Conversion of carbon monoxide as a function of time on stream for oxygen- and nitrogen-annealed cobalt-substituted YBCO perovskites. (○) $YBa_2Cu_{3-\delta}Co_\delta^{ox}O_{6+x}$, $\delta = 0.12$, 240°C; (□) $YBa_2Cu_{3-\delta}Co_\delta^{ox}O_{6+x}$, $\delta = 0.24$, 240°C; (●) $YBa_2Cu_{3-\delta}Co_\delta^{red}O_{6+x}$, $\delta = 0.12$, 200°C.

TABLE 1

Oxygen Content by Titration of Fresh and Used $YBa_2Cu_{3-\delta}Me_\delta O_{6+x}$ Catalysts Annealed in Oxygen (Me^{ox}) and in Nitrogen (Me^{red}), Substituent Content by XPS, and Rate of CO Oxidation

Me	δ		x		Rate (μmol/m^{2}min)
	As prep.	By XPS	Before use	After use[a]	
None^{ox}	0				45.3[b]
None^{red}	0				60.5[b]
Co^{ox}	0.12		0.61	0.51	29.2
	0.24		0.64	0.52	15.6
	0.36		0.67	0.53	13.7
	0.48		0.80	0.57	8.0
Co^{red}	0.12	0.04	0.48	0.35	29.3
	0.24	0.24	0.50	0.46	24.1
	0.36	0.33	0.58	0.48	18.4
	0.48	0.42	0.59	0.58	4.5
Al^{ox}	0.12		0.53	0.36	37.3
	0.24		0.56	0.52	45.1
	0.36		0.71	0.63	35.0
	0.48		0.75	0.67	35.2
Al^{red}	0.12	0.03	0.39	0.34	47.1
	0.24	1.23	0.50	0.45	17.1
	0.36	0.61	0.59	0.42	34.3
	0.48	0.58	0.60	0.50	31.0

[a] Used at 240°C and p_{O_2} = 166 Torr for Me^{ox}, and at 200°C and p_{O_2} = 8 Torr for Me^{red}.

[b] Calculated for conditions as in [a] using the rate equation in Ref. (*16*).

up of an intergrowth sequence with $-CuO_2-|BaO-CuO_x-BaO|-CuO_2-Y$ sheets along the *c*-axis. Al and Co are believed to substitute at CuO_x positions which seem to affect oxidation catalysis (*13*). Therefore, the CuO_x sheet will be described more with respect to ideal oxygen filling, ordering of vacancies, and substitution of Cu. We denote the sheet as –Cu–( )–Cu–, where ( ) can be an oxygen species O or an oxygen vacancy [ ]. In the highly ordered structure with $x = 1$, all the anion positions along the *b*-axis are occupied by oxygen and the coordination around Cu is square planar. These oxygen atoms are mobile and can leave the structure at elevated temperatures. At $x = 0.5$, half of these oxygen atoms have left and an ordering in which –O–Cu–O– chains alternate with –[ ]–Cu–[ ]– chains along the *a*-axis is observed. In this case half of the Cu atmos are in two-fold linear coordination and of formal valence +1. When all these oxygens have left, at $x = 0$, all Cu are in twofold linear coordination. When these Cu atoms are replaced with Co or Al, more oxygen species will be coordinated to the latter cations to maintain their higher oxidation states. Thus, when the cations are in 3+ oxidation states, oxygen will be additionally ordered along the *a*-axis. This may lead to orthorhombic-to-tetragonal transitions at $0.7 < x < 1.3$, e.g., for Co substitution $\delta = 1$ (*25*). But when $\delta = 0.5$ and $0 < x < 0.7$, orthorhombic-to-tetragonal transitions can possibly occur due to disordered but equal distribution of oxygen along *a* and *b* axes. The *x*-values and δ for most of the samples, cf. Table 1, are within the ranges in which the ordering of oxygen can be described as disordered, but equal along the *a* and *b* axes. Some consequences arising from this may be the following. Due to the low δ-value, the amount of oxygen actually added additionally to the

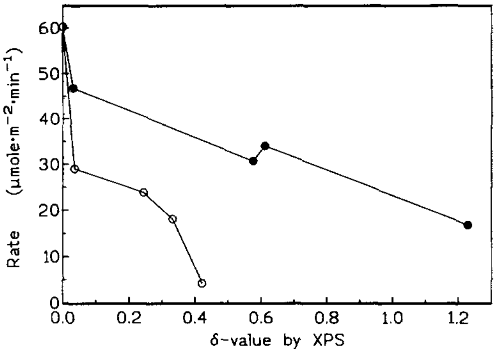

FIG. 4. Rate of carbon monoxide oxidation over nitrogen-annealed cobalt- and aluminium-substituted YBCO perovskite as a function of degree of substitution as measured by XPS: 200°C, p_{CO} = 4 Torr, p_{O_2} = 16 Torr). (○) $YBa_2Cu_{3-\delta}Co_\delta^{red}O_{6+x}$; (●) $YBa_2Cu_{3-\delta}Al_\delta^{red}O_{6+x}$.

material when compared to YBCO may be small. The coordination around the substituent cations may then stabilize lower oxidation states for Co, while for Al unfavorable coordination can lead to structural distortion and segregation of phases in accordance with XPS data (see Table 1).

Considering surface compositions, XPS results show that fresh Co-substituted samples have compositions which are fairly close to those of the bulk, but for the Al samples the δ-values differ considerably; cf. Table 1. These results together with those of the X-ray diffraction seem to further support the view that Co may be stabilized in the lower valence state, while Al is segregated. The data also indicate changes in the surface structures containing Cu^{2+} and Cu^{1+} species, as is evident from the Cu 2p spectra and the satellite-to-main line intensity ratios. It is worthy of mention that even at the lowest oxygen pressure applied, the formation of Cu^{1+} is low compared to that during (amm)oxidation of toluene (*6*, *11*, *12*), where it is exclusively Cu^{1+}.

Surface Influences on Activity

Co-substituted samples appeared to be homogeneous by XRD and XPS, and the large drop in activity, cf. Table 1 and Figs. 1 and 4, at increasing Co content strongly suggests that segregation of a separate Co phase does not occur. In such a case, very probably, an opposite effect would have been obtained since the activity over Co_3O_4 is considerably higher than over CuO. A plausible explanation of the activity pattern of the Co samples is that Co and Cu form surface compounds or structures in which the coordination around each Co cation favors an oxidation state close to 2+. In this situation, Co sites will be less active for CO oxidation as observed for tetragonally coordinated Co^{2+} species (*26*). Consequently, the gradual replacement of active –Cu–O–Cu– sites with less active –Cu–O–Co(II)– sites can explain the decreased activity with Co substitution.

The somewhat different activity pattern observed for Al-substituted samples can be explained considering that Al is possibly segregated out of the bulk, indicated by XPS, leaving more –Cu–O–Cu– and –Cu–( )–Cu– species at the surface. If activity is plotted against δ-value measured by XPS for reduced samples, a better correlation is obtained, see Fig. 4, since $Al_{0.48}$ then has the highest δ-value.

Bulk Influences on Activity

Considering the mobility of lattice oxygen species, the ordering of oxygen at the surface, i.e., occupation of the –Cu–( )–Me–position, will depend on the changes at near-surface and bulk regions. It seems that when these positions are filled, and also when near-surface vacancies are filled, the catalytic activity is low. In the opposite situation the activity is higher. Compare the lower activity of oxygen-annealed samples than of nitrogen-annealed samples; cf. Table 1 and Figs. 1 and 2. However, the transitory stages, see Fig. 3, appear to develop higher activity. For preoxidized $YBCMe^{ox}$ samples, the activity increases in the absence of oxygen, since –Cu–( )–Cu– is gradually created, but passes through an optimum after the surface is probably depleted of mobile oxygen species. When oxygen is reintroduced, the activity initially increases and later decreases with

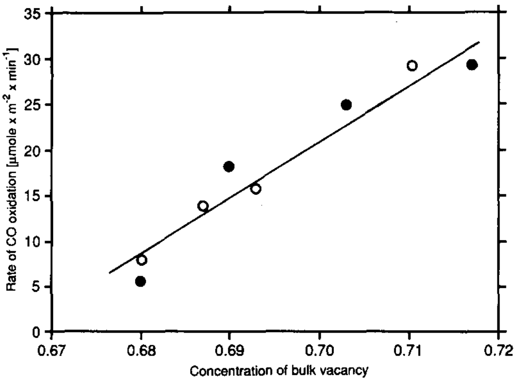

FIG. 5. Rate of CO oxidation as a function of concentration of bulk vacancy derived after normalizing the compositions based on titration results to a basic perovskite ABX_3 structure; e.g., for $YBa_2Cu_{3-\delta}Co_\delta O_{6+x}$, $\delta = 0.12$, $A = Y_{0.33}Ba_{0.67}$, $B = Cu_{0.96}Co_{0.04}$, and $X = O_{2.20}[\ ]_{0.80}$, where [ ] is a vacancy. (○) $YBa_2Cu_{3-\delta}Co_\delta^{ox}O_{6+x}$, 240°C, p_{CO} = 4 Torr, p_{O_2} = 166 Torr; (●) $YBa_2Cu_{3-\delta}Co_\delta^{red}O_{6+x}$, 200°C, p_{CO} = 4 Torr, p_{O_2} = 16 Torr.

time as –Cu–( )–Cu– and near-surface vacancies become filled up. In the case of YBCMe^{red}, pretreated in nitrogen, when used initially at high oxygen pressure, there is a tendency for –Cu–( )–Cu– and near-surface positions to be filled with oxygen, thus rendering these sites less active. At the later decreased oxygen concentration, the activity therefore increases again as the sites are depleted with oxygen.

If the response to the step changes were confined to a thin surface layer, one might expect that the responses would be immediate. As this is not the case it is likely that bulk processes are also of importance. There may be an equilibrium between the surface and bulk concentration of vacancies. The bulk oxygen content can affect reactivity by controlling the rate of oxygen migration into and out of the bulk, and also the occupation of the surface –Cu–( )–Cu– positions. It has been found that the in-diffusion of oxygen is strongly dependent on the x-value, whereas the out-diffusion is not (*27*). At high bulk oxygen content the concentration of vacancies in the bulk and near-surface region is low. In this situation dissociative oxygen adsorption will be limited, yielding low reactivity. At low bulk oxygen content, the concentration of bulk vacancies and –Cu–( )–Cu– species is high, and will increase the rate of migration and dissociation of oxygen at the surface. The high concentrations of –Cu–( )–Cu– and reactive O^- species will lead to a high rate of oxidation. Support for these views, cf. Fig. 5, is the almost linear dependence of CO oxidation rate on the bulk concentration of vacancies derived after normalizing compositions in Table 1 to a basic perovskite structure of ABX_3. For Me^{ox} and Me^{red} samples the bulk is respectively neither fully reduced nor fully oxidized and this depends on the reaction at the surface.

ACKNOWLEDGMENT

Financial support from the National Energy Administration (STEV) is acknowledged.

REFERENCES

1. Holland G. F., and Stacy, A. M., *Acc. Chem. Res.* **21,** 8 (1987).

2. Grant, P. M., *Progr. High Temp. Supercond.* **20,** 1 (1989).

3. Grant, P. M., *Adv. Mater.* **2,** 232 (1990).

4. Hansen, S., Otamiri, J. C., Bovin, J.-O., and Andersson, A., *Nature* **334,** 143 (1988).

5. Otamiri, J. C., Andersson, A., Hansen, S., and Bovin, J.-O., *in* "New Developments in Selective Oxidation, Studies in Surface Science and Catalysis" (G. Centi and F. Trifirò, Eds.), Vol. 55, p. 275. Elsevier, Amsterdam, 1990.

6. Otamiri, J. C., Andersson, S. L. T., and Andersson, A., *Appl. Catal.* **65,** 159 (1990).

7. Jiang, A., Peng, Y., Zhou, Q., Gao, P., Yuan, H., and Deng, J., *Catal. Lett.* **3,** 235 (1989).

8. Mizuno, N., Yamato, M., and Misono, M., *J. Chem. Soc. Chem. Commun.*, 887 (1988).

9. McCarty, J. G., Quinlan, M. A., and Wise, H., *in* "Proceedings, 9th International Congress on Catalysis, Calgary, 1988" (M. J. Phillips and M. Ternan, Eds.), Vol. 4, p. 1818. Chem. Inst. Canada, Ottawa, 1988.

10. Lee, I., and Ng, K. Y. S., *Catal. Lett.* **2,** 403 (1989).

11. Otamiri, J. C., Andersson, A., Andersson, S. L. T., Crow, J. E., and Gao, Y., *J. Chem. Soc. Faraday Trans.* **87,** 1265 (1991).

12. Andersson, S. L. T., *J. Chem. Soc. Faraday Trans.* **88,** 83 (1992).

13. Hansen, S., Otamiri, J. C., and Andersson, A., *Catal. Lett.* **6,** 33 (1990).

14. Mizuno, N., Toyama, H., Tanaka, M., Yamato, M., and Misono, M., *Bull. Chem. Soc. Jpn.* **64,** 1383 (1991).

15. Halasz, I., Brenner, A., Shelef, M., and Ng, K. Y. S., *Catal. Lett.* **1,** 327 (1991).

16. Otamiri, J. C., and Andersson, S. L. T., *Appl. Catal.* **73,** 267 (1991).

17. Salvador, P., and Fierro, J. L. G., *J. Solid State Chem.* **81,** 240 (1989).

18. Andersson, S. L. T., and Otamiri, J. C., *Appl. Surf. Sci.* **45,** 1 (1990).

19. Dauth, B., Sen, P., Rupp, B., Gudat, W., Ziegler, Ch., and Göpel, W., *Z. Phys. B* **79,** 169 (1990).

20. Dai, Y., Manthiram, A., Campion, A., and Goodenough, J. B., *Phys. Rev. B* **38,** 5091 (1988).

21. Iqbal, Z., Leone, E., Chin, R., Signorelli, A. J., Bose, A., and Eckhardt, H., *J. Mater. Res.* **2,** 768 (1987).

22. Wang, W., Tian, L., Gong, Y., and Sun, Y., *Surf. Sci.* **213,** 303 (1989).

23. Gang, X., Ciepak, M. Z., Gavrin, A., Streitz, F. H., Bakhshi, A., and Chien, C. L., *Phys. Rev. Lett.* **60,** 144 (1988).

24. Gang, X., Ciepak, M. Z., Musser, D., Gavrin, A., Streitz, F. H., Chien, C. L., Rhyne, J. J., and Gotaas, J. A., *Nature* **322,** 238 (1988).

25. Tao, Y. K., Swinnea, J. S., Manthiram, A., Kim, J. S., Goodenough, J. B., and Steinfink, H., *J. Mater. Res.* **3,** 248 (1988).

26. Boreskov, G. K., *in* "Proceedings, 6th International Congress on Catalysis, London, 1976" (G. C. Bond, P. B. Wells, and F. C. Tompkins, Eds.), Vol. 1, p. 204. Chemical Society, London, 1977.

27. Tu, K. N., Yeh, N. C., Park, S. I., and Tsuei, C. C., *Phys. Rev. B* **39,** 304 (1989).